# Enhancing the Static and Dynamic Performance of High-Speed VCSELs by Zn-Diffused Shallow Surface Relief Apertures

Zuhaib Khan, Jia-Liang Yen, Chen-Lung Cheng, Kai-Lun Chi, and Jin-Wei Shi, *Senior Member, IEEE*

***Abstract*— In this paper, we demonstrate a novel structure for 850- and 940-nm wavelength high-speed vertical-cavity surface-emitting lasers (VCSELs). Extra shallow apertures (∼20 nm) are etched on the topmost current spreading (CS) layer of 850- or 940-nm VCSELs, which have Zn-diffusion and oxide-relief apertures inside. Such a structure simultaneously allows a significant enhancement of the output power and a reduction in the number of optical modes in the optical spectrum, which migrates toward the quasi-single-mode (QSM). Comparison is made to multi-mode (MM) reference VCSELs produced without etching of the CS layer. The etched devices exhibit a larger signal-to-noise ratio for error-free 32 Gbit/s transmission over 100-m MM fibers (MMFs) at both wavelengths (850 and 940 nm). In addition, the dynamic/static performance of the etched samples is also superior to that of a QSM reference sample, produced by utilizing only Zn-diffusion apertures without etching of the CS layer. The demonstrated device structure opens the door to greatly improve the performance of SM and high-power VCSELs for high-speed data transmission.**

***Index Terms*— Semiconductor lasers, vertical cavity surface emitting lasers.**

## I. Introduction

HIGH-SPEED vertical-cavity surface-emitting lasers (VCSELs) that can operate in the wavelength window from 850 to around 1000 nm have lately attracted a lot of attention due to their suitability for optical interconnect (OI) applications [1]–[10]. Modern data centers and high-performance computing (HPC) systems require millions of OI channels [10]. Shortwave wavelength division multiplexing (SWDM) [9], [10], driven by VCSELs operating in the 850-1000 nm wavelength window, has been adapted to further enhance the package density and reduce the number of costly multi-mode fibers (MMFs) needed in an OI system. For a four channel SWDM system, a total data transmission rate of nearly 200 Gbit/sec has been demonstrated [8], [10].

Manuscript received June 15, 2018; revised August 21, 2018; accepted September 5, 2018. Date of publication September 13, 2018; date of current version September 18, 2018. This work was supported by the Ministry of Science and Technology in Taiwan under Grants MOST 106-2221-E-008 -063 -MY3 and MOST 107-2622-E-008 -002 -CC2. *(Corresponding author: Jin-Wei Shi.)*

Z. Khan, C.-L. Cheng, K.-L. Chi, and J.-W. Shi are with the Department of Electrical Engineering, National Central University, Taoyuan City 320, Taiwan (e-mail: jwshi@ee.ncu.edu.tw).

J.-L. Yen is with the Department of Information Technology, Takming University of Science and Technology, Taipei 114, Taiwan.

Color versions of one or more of the figures in this paper are available online at http://ieeexplore.ieee.org.

Digital Object Identifier 10.1109/JQE.2018.2869746

The target for the next generation of interconnect frameworks is a data rate per channel of 56 Gbit/sec (CEI (Common Electrical Interface)-56G) [1]–[5], [10] with a total data rate of up to 400 Gbit/sec. Complex modulation/de-modulation techniques, such as pulse-amplitude modulation (PAM) [11], orthogonal frequency-division multiplexing (OFDM) [12], and feed forward equalization (FFE) [1], [13] have been applied to alleviate the speed bottleneck for VCSELs under direct modulation.

However, using any of the afore-mentioned techniques to boost the data rate makes the power budget in the linking channel even more critical. It is thus important to design VCSELs which simultaneously offer high modulation-speeds, high slope-efficiency, and enough output power to meet the requirements of the next-generation of OI.

Furthermore, the demand for OI channels with linking distances as long as or exceeding 2 km (Spec. of LR4 2km Lite [14]) is booming because of the rapid increase in the number and size of warehouse-scale data centers created to satisfy the relentless growth of global internet traffic. The production of enough output power from the VCSELs thus becomes a critical issue to compensate for the significant optical transmission loss over km long MMFs [14]. Having 850-1000 nm VCSELs with linking distances up to the km range and capable of very-high data rate (>50 Gbit/sec) transmission would allow the MMF infrastructure installed at these data centers to function without wavelength conversion to 1.3-1.55 $\mu$m for long-reach single-mode fiber (SMF) transmission [14]–[17]. Furthermore, producing a seamless VCSEL driven MMF network would not only reduce the cost, latency, and energy consumption but also alleviate the need for wavelength conversion. One of the most effective ways to extend the linking distance to the km level is to reduce the optical linewidth of the high-speed MM VCSELs to produce quasi single-mode (or single-mode) output [14]–[18]. This can be realized by aggressively downscaling the oxide aperture size to less than ∼3 $\mu$m for 850 nm VCSELs [5]. However, their SM power is limited and is too small to meet the required power budget for the advanced modulation format discussed above. Several VCSEL structures for attaining higher SM power have been reported, including Zn-diffusion [14], [15], surface relief [16], [17], and anti-guide (leaky) cavity [18] structures. However, it is necessary to incorporate extra intra-cavity loss into these VCSEL structures in order to suppress the

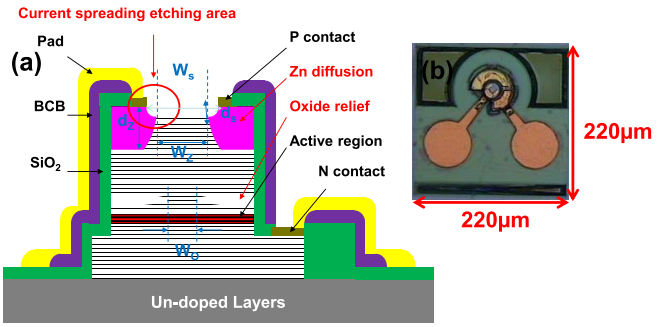


Fig. 1. (a) Conceptual cross-sectional view and (b) top-view of the demonstrated VCSELs.

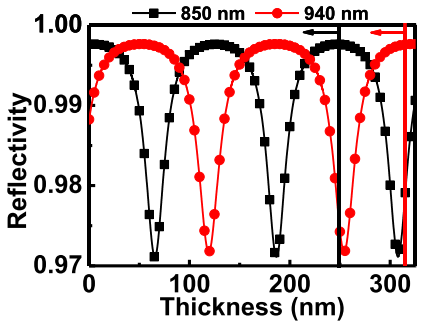


Fig. 2. Simulated reflectivity of top DBR mirror versus thickness of the CS layer for 850 (black line) and 940 (red line) nm VCSELs. The black and red vertical lines indicate the as grown CS layer thickness of real devices. The arrow head represent the decrease in CS layer thickness.

higher-order mode lasing which usually results in an increase in the threshold current and the degradation in the differential quantum efficiency with the modulation speed as compared to those of the MM reference [14].

In this work, we demonstrate a novel VCSEL structure emitting at the 850 and 940 nm wavelengths. The static and high-speed transmission performance of this high-speed VCSEL with Zn-diffusion and oxide-relief apertures inside can be simultaneously improved by etching extra apertures with a shallow depth (∼20 nm) into the topmost current spreading (CS) layer. This VCSEL structure allows for a significant enhancement in the output power and reduction in the number of optical modes in the optical spectrum, which migrates toward quasi single-mode (QSM) operation. The control device exhibits superior transmission performance over 100 meter multi-mode fibers (MMFs) at both wavelengths (850 and 940 nm) compared to the MM reference samples without the etched apertures. The demonstrated device structure opens up new ways to greatly improve the performance of SM and high-power VCSELs for high-speed data transmission.

## II. Device Structure

Here, VCSELs with two different central wavelengths (850 and 940 nm) are studied. For a detailed description of their structure, which includes Zn-diffusion and oxide-relief apertures, please refer to [5]. Figure 1 (a) shows a conceptual cross-sectional view of the VCSEL structures studied here. As can be seen, the major difference between this newly demonstrated structure and the previous ones is the incorporation of additional surface relief apertures ($W_s$), which are realized by shallow etching of the topmost current spreading (CS) layer, above the Zn-diffusion ($W_z$) aperture. According to our calculations, etching of the CS layer with apertures of a proper thickness will decrease the reflectivity of the top distributed-Bragg reflector (DBR) mirror and lead to an increase in the output power [7]. In addition, the extra scattering loss induced by the side-walls etched in the Zn-diffusion region, encircled in red in Figure 1, further enhances the selectivity between the fundamental and transverse cavity modes in our VCSEL structure. Figure 2 shows the simulated reflectivity of the top DBR mirrors of our 850 and 940 nm VCSEL structures versus the thickness of the current spreading CS layer. As can be seen, only a slight change in the thickness of the CS layer can a lead

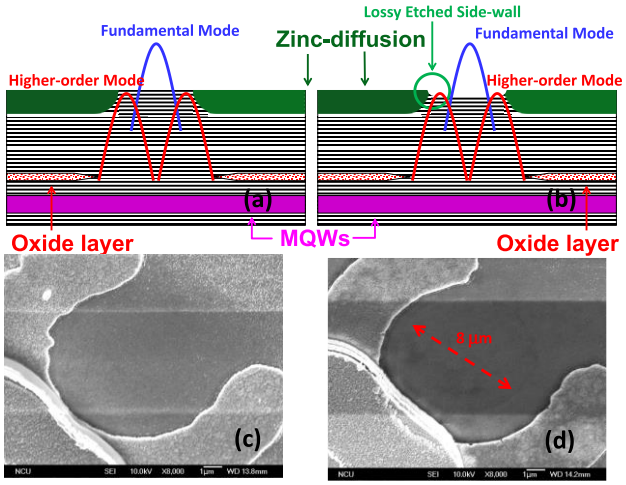


Fig. 3. Conceptual cross-sectional views of optical modes inside a Zn-diffused VCSEL cavity (a) with and (b) without shallow surface relief apertures. The SEM top-view image of VCSELs (c) with and (d) without shallow surface relief apertures.

to a significant change in the reflectivity, which can be used to control the photon lifetime and output power of the studied VCSEL structures [7]. The working principles of the proposed device structure are illustrated in Figures 3 (a) and (b). As can be seen, the far-field pattern of the higher order mode in the VCSEL cavity is usually doughnut-shaped, with a large overlap with the Zn-diffused region. Compared with the VCSEL structure with only Zn-diffusion apertures, there is an increase in the threshold gain of the higher order mode in our demonstrated structure due to the combination of the Zn-induced free-carrier absorption loss [11] and the extra scattering loss from the etched surface and side-walls. Overall, the incorporation of additional surface-relief apertures into the structure of our Zn-diffusion VCSEL, leads to a higher output power together with a larger side-mode suppression ratio. Figures 3 (c) and (d) show scanning electron microscopic (SEM) top-views of the light-emission apertures of VCSELs fabricated without and with surface-relief etching, respectively. A clear disk-shaped pattern on the topmost CS layer can be observed in the etched device. The working principles of our device are very different from those of VCSELs fabricated with only surface-relief apertures for single-mode

performance as reported in [16]. In the center of the light emission aperture of the traditional surface-relief structure, it is necessary to precisely etch an extra anti-phase quarter wavelength layer to reduce the mirror loss (required threshold gain) in the fundamental mode. Precise control of the etching depth and e-beam lithography for alignment between the surface-relief and oxide apertures are usually necessary [16]. In contrast, no such additional anti-phase quarter wavelength layer is required in our structure. The selectivity between the fundamental mode and higher order modes is mainly achieved by the Zn-diffusion apertures. Compared to the surface-relief approach, the Zn-diffusion device offers higher single-mode power (7.2 vs. 6.5 mW) and lower differential resistance without needing to precisely control the etching depth and using e-beam lithography [19]. Nevertheless, both these structures suffer from the problem of increased intra-cavity loss and threshold current. The major contribution of this new structure is that such two techniques (Zn-diffusion + surface-relief) are combined to produce a device which demonstrates superior dynamic/static performance to that of the QSM reference sample with only Zn-diffusion apertures. This will be discussed in greater detail later.

The epi-layer structures for the 850 and 940 nm VCSELs, purchased from LandMark,[1] were grown on semi-insulating GaAs substrates. In order to attain very high-speed modulation, a short-cavity structure, with a cavity length of 1/2 $\lambda$ was adopted in our device, where $\lambda$ is the Bragg wavelength inside the VCSEL cavity. Such a design can shorten the internal carrier transit time, increase the optical confinement in the active layers, and further enhance the 3-dB E-O bandwidth [3] of the VCSEL. The active layers of the 850 and 940 nm VCSELs are composed of three $In_{0.08}Ga_{0.92}As/Al_{0.35}Ga_{0.65}As$ (50/80Å) and $In_{0.3}Ga_{0.7}As/Al_{0.35}Ga_{0.65}As$ (40/80Å) MQWs, respectively. The 850 (940) nm MQWs are sandwiched between 38-pair n-type and 19-pair p-type $Al_{0.9}Ga_{0.1}As/Al_{0.12}Ga_{0.88}As$ ($Al_{0.9}Ga_{0.1}As/Al_{0.05}Ga_{0.95}As$) Distributed-Bragg-Reflector (DBR) layers. VCSELs for both wavelengths have the same $Al_{0.98}Ga_{0.02}As$ layer thickness (50 nm) above the MQWs for oxidation. The bulk p-type $Al_xGa_{1-x}As$ layer above the p-type DBRs in both VCSEL structures serves as a current spreading (CS) layer to further reduce the differential resistance. The aluminum (Al) mole fraction (x) and thickness of the CS layer for the 850 (940) nm VCSELs are 0.1 (0.05) and 0.25 (0.315) $\mu$m, respectively. Here, the thickness of the CS layer is chosen to maximize the top DBR reflectivity to be around 99.7%. The aperture sizes and depths of each studied device are specified in the figure captions.

## III. Measurement Results and Discussion

Three kinds of device structure were fabricated. All of them (structures A to C) had the same sized oxide-relief ($W_o$), Zn-diffusion ($W_z$) apertures, surface relief apertures ($W_s$), and Zn-diffusion depth ($d_z$), specifically 6,7,8, and 1 $\mu$m, respectively. The only difference between them was the thickness of the CS etching layer ($d_s$) which was 0, 20, and 25 nm, for Structures A to C, respectively.

[1]LandMark Optoelectronics Corporation, No.12, Nanke 9th Rd., Shanhua Dist., Tainan City 741, Taiwan.

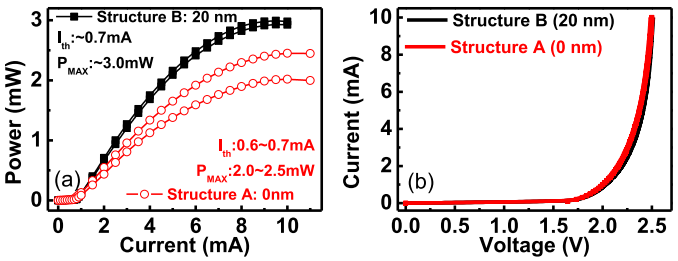


Fig. 4. Measured (a) L-I and (b) I-V curves for 850 nm VCSELs with structures A ($d_s$ = 0 nm) and B ($d_s$ = 20 nm). ($W_z/W_o/W_s/d_z$) = 7/6/8/1 $\mu$m.

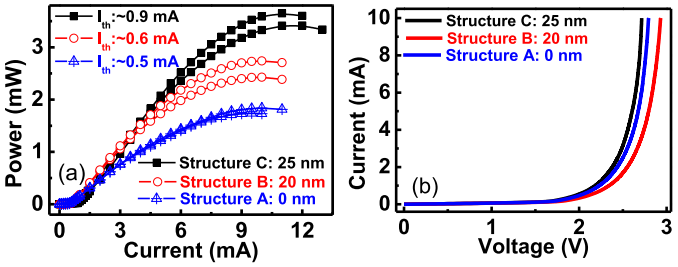


Fig. 5. Measured (a) L-I and (b) I-V curves for 940 nm VCSELs with Structures A ($d_s$ = 0 nm), B ($d_s$ = 20 nm), and C ($d_s$ = 25 nm). ($W_z/W_o/W_s/d_z$) = 7/6/8/1 $\mu$m.

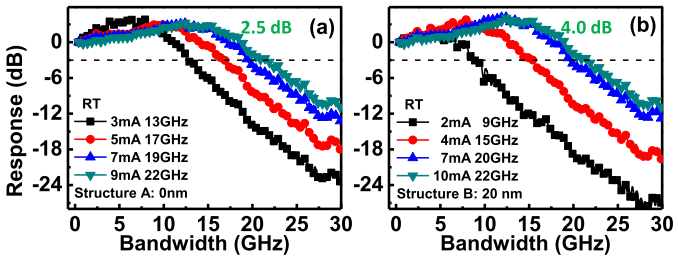


Fig. 6. Measured bias dependent electrical-to-optical (E-O) frequency responses of 850 nm VCSELs with (a) Structure A ($d_s$ = 0 nm) and (b) Structure B ($d_s$ = 20 nm). ($W_z/W_o/W_s/d_z$) = 7/6/8/1 $\mu$m. The peak magnitude (green word) in the E-O responses is specified.

Figures 4 and 5 show the measured L-I and V-I curves for the 850 and 940 nm VCSELs, respectively, with the three different structures (A to C). As can be seen, all have similar I-V characteristics for both wavelengths, which indicates that the surface relief process does not lead to degradation of the Ohmic contact performance. In addition, although Structure C has a slightly larger $I_{th}$ than either A or B, it comes with the highest differential quantum efficiency and output power among these three structures due to having the smallest mirror reflectivity (largest $d_s$), as expected.

Figures 6 to 9 show the measured bias dependent electrical-to-optical (E-O) frequency responses and electroluminescence spectra for the 850 and 940 nm VCSELs with different structures (A to C). Here, we measured the E-O responses for several devices with each structure; the E-O frequency responses shown in these figures are just the representative ones, which are the most often measured traces for the corresponding device structure. In addition, the magnitude (dB) of the peak

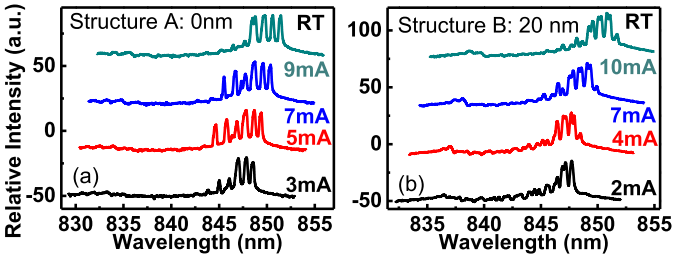


Fig. 7. Measured bias dependent output optical spectra of 850 nm VCSELs with (a) Structure A ($d_s$ = 0 nm) and (b) Structure B ($d_s$ = 20 nm). ($W_z/W_o/W_s/d_z$) = 7/6/8/1 $\mu$m.

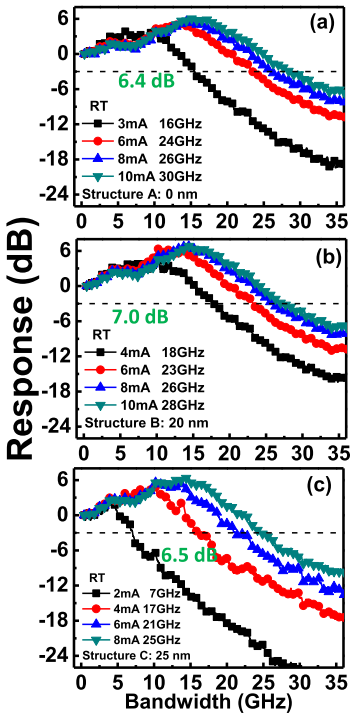


Fig. 8. Measured bias dependent electrical-to-optical (E-O) frequency responses of 940 nm VCSELs with (a) Structure A ($d_s$ = 0 nm), (b) Structure B ($d_s$ = 20 nm), and (c) Structure C ($d_s$ = 25 nm). ($W_z/W_o/W_s/d_z$) = 7/6/8/1 $\mu$m. The peak magnitude (green word) in the E-O responses is specified.

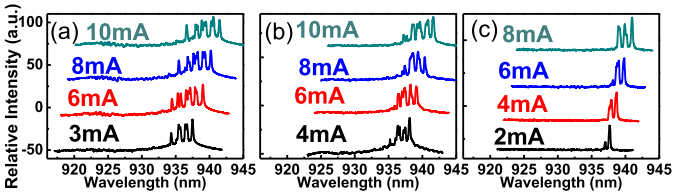


Fig. 9. Measured bias dependent output optical spectra of 940 nm VCSELs with (a) Structure A ($d_s$ = 0 nm), (b) Structure B ($d_s$ = 20 nm), and (c) Structure C ($d_s$ = 25 nm). ($W_z/W_o/W_s/d_z$) = 7/6/8/1 $\mu$m.

E-O response due to relaxation of the oscillations is specified for each trace. We can clearly see that by the incorporation of surface relief apertures into our Zn-diffusion VCSELs (both wavelengths), we can not only increase the output power but also reduce the number of optical modes in the measured spectra allowing it to migrate towards the characteristics of

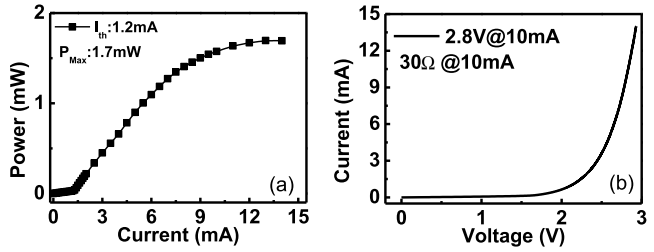


Fig. 10. Measured (a) L-I and (b) I-V curves of 940 nm VCSELs with structure A ($d_s$ = 0 nm). ($W_z/W_o/d_z$) = 7/9/2.1 $\mu$m.

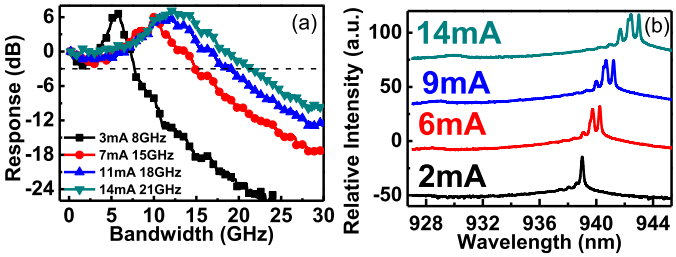


Fig. 11. Measured bias dependent (a) electrical-to-optical (E-O) frequency responses and (b) output optical spectra of 940 nm VCSELs with Structure A ($d_s$ = 0 nm). ($W_z/W_o/d_z$) = 7/9/2.1 $\mu$m.

quasi-SM. Although improvements in the static performance of these surface relief devices are observed, there is a gradual degradation in the measured 3-dB E-O bandwidths with the increase of $d_s$ for the 940 nm VCSELs. Such a degradation in speed performance can be attributed to the increase in the mirror loss and threshold current ($I_{th}$), which increases the bias current essential for high-speed operation and results in more serious device heating.

However, for the traditional Zn-diffusion (Quasi-) SM VCSEL [11], both its maximum output power and speed are simultaneously sacrificed for SM performance as compared to those of the MM reference device due to the significant Zn-induced intra-cavity loss. Figures 10 and 11, respectively, show the measured L-I-V curves and bias dependent E-O frequency responses/electroluminescence spectra of (Quasi-) SM (QSM) 940 nm VCSELs with structure A (no surface relief). In order to attain (Quasi-) SM performance in this device, the size of $W_o$ must be larger than $W_z$ (9 vs. 7 $\mu$m) and the $d_z$ must be increased from 1 to 2.1 $\mu$m to have significant intra-cavity loss [14]. Details about the geometric size are given in the figure caption. Comparison with the measurement results for the 940 nm VCSEL with structure C reveals a very similar QSM performance, as shown in Figure 9. We can clearly see that both the static and dynamic performance can be greatly improved by implementing extra surface relief apertures above the Zn-diffusion layer.

Due to the improvement in the static performance, an enhanced transmission performance can be expected. In our transmission setup, a 32 Gbit/s non-return-to-zero (NRZ) electrical signal with a pseudo-random binary sequence (PRBS) length of $2^{15} - 1$ is generated through the pattern generator to drive the VCSELs being tested. A lens fiber tip is used to collect the modulated light output from the VCSEL

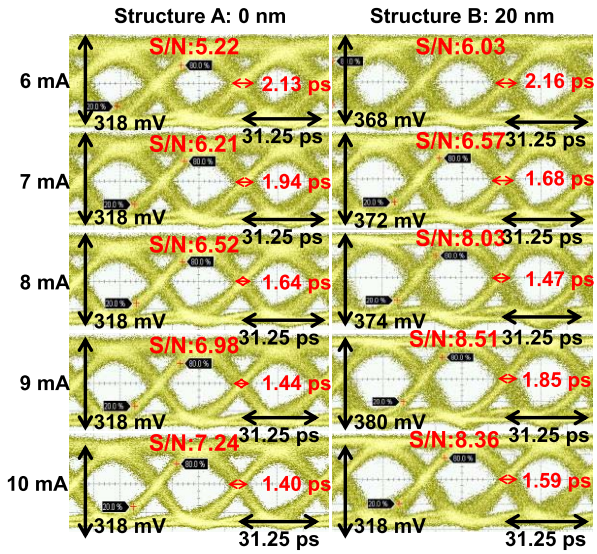


Fig. 12. Measured 32 Gbit/sec transmission results through a 1 meter OM5 MMF (BTB) using the 940 nm VCSELs with Structures A ($d_S = 0$ nm) and B ($d_S = 20$ nm) under different bias currents. ($W_Z/W_O/W_S/d_Z$) = 7/6/8/1 $\mu$m.

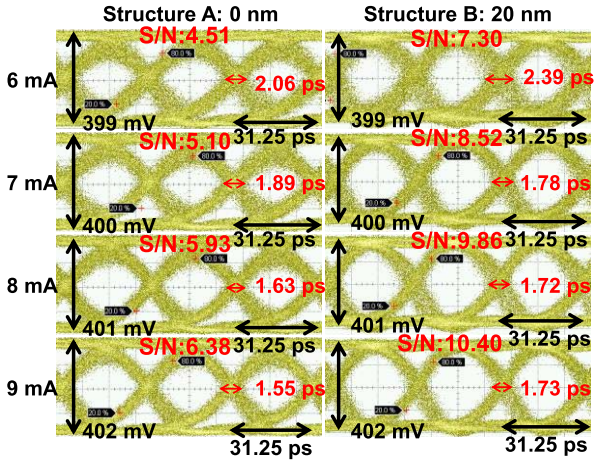


Fig. 13. Measured 32 Gbit/sec transmission results through a 100 meter OM4 MMF using the 850 nm VCSELs with Structures A ($d_S = 0$ nm) and B ($d_S = 20$ nm) under different bias currents. ($W_Z/W_O/W_S/d_Z$) = 7/6/8/1 $\mu$m.

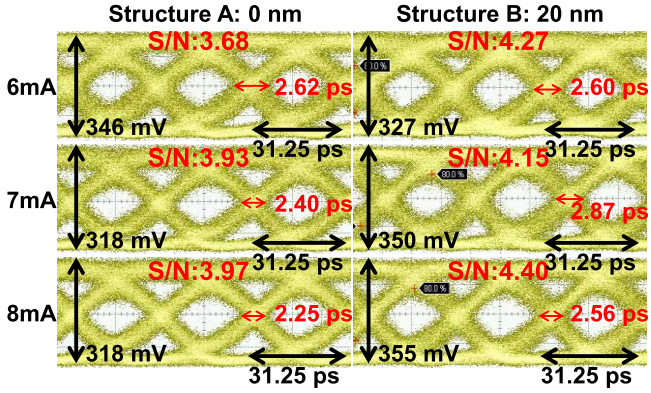


Fig. 14. Measured 32 Gbit/sec transmission results through a 100 meter OM5 MMF using the 940 nm VCSELs with Structures A ($d_S = 0$ nm) and B ($d_S = 20$ nm) under different bias currents. ($W_Z/W_O/W_S/d_Z$) = 7/6/8/1 $\mu$m.

during testing. In addition, OM4 and OM5 MMFs, which are optimized for 850 and 940 nm wavelength transmission, respectively, are adopted in our setup. At the receiving end, a high-speed photoreceiver module (D50-1300M; VI-system)[1], which can cover the 840 to 1550 nm optical wavelengths for an optical-to-electrical (O-E) bandwidth in excess of 23 GHz 3-dB across this wide optical operation window, is used. Figure 12 shows the 32 Gbit/sec transmission results obtained with the 940 VCSELs (for structures A and B) after 1 meter (back-to-back (BTB)) MMF transmission. We can clearly see that both structures (A and B) allow error-free transmission performance. In addition, the S/N ratios values of the measured eye-patterns of structure B are larger than those of structure A. The improved transmission performance is due to further enhancement of the differential quantum efficiency and output power arising from the extra surface relief apertures of our devices, as illustrated in Figures 4 and 5. However, structure B suffers from a slightly larger timing jitter in the measured eye patterns than does structure A. This phenomenon can be attributed to the lower DBR reflectivity in structure B which reduces the photon lifetime and enhances the relaxation oscillation in the measured E-O frequency response [20]. As can be clearly seen in Figures 6 and 8, the relaxation oscillation induced peaking in the measured E-O frequency responses is more pronounced in the measured traces for structure B than that shown in the measured traces for structure A. Under a large VCSEL signal modulation, a highly damped E-O frequency response with a sufficient 3-dB E-O bandwidth is preferred to get high-quality eye-patterns [20]. Figures 13 and 14 show the 32 Gbit/sec transmission results for 850 and 940 VCSELs (with structures A and B) after 100 meter MMF transmission. Similar to the case of BTB transmission, structure B shows superior transmission results to A due to its improved static performance, which includes a narrower optical spectral width and less optical modal dispersion. Theoretically speaking, the 940 nm VCSEL with structure C should have the best transmission performance among all the device structures studied here due to its QSM performance and because it suffers from the least amount of modal dispersion during transmission [14]–[18]. However, the measurement results for Structure C are not consistent with the above. In comparison to the MM reference, the QSM device should be more sensitive to optical feedback during high-speed data transmission [21], which would lead to a serious degradation in the eye quality. In order to minimize this effect, it is necessary to use a lens fiber with a good anti-reflection (AR)-coating on its tip for VCSEL output light collection. However, an AR-coated lens fiber was only used at 850 nm. In order to study the transmission performance of Structure C for 940 nm optical wavelength operation, it is necessary to make further improvements in our measurement setup, which is a goal of future work.

## IV. Conclusion

In this work we demonstrate a novel VCSEL structure for attaining high-power, high-speed quasi-SM performance. The implementation of an extra shallow surface relief aperture

layer on top of Zn-diffusion VCSELs allows these devices to exhibit higher output power, larger differential quantum efficiency, narrower optical spectral width, and better 32 Gbit/sec high-speed transmission performance over 100 meter MMFs than those of reference samples without the surface relief apertures.

## REFERENCES


[1] R. Puerta *et al.*, "107.5 Gb/s 850 nm multi- and single-mode VCSEL transmission over 10 and 100 m of multi-mode fiber," in *Proc. Post-deadline Papers OFC*, Anaheim, CA, USA, Mar. 2016, pp. 1–3, Paper Th5B.5.

[2] D. M. Kuchta *et al.*, "A 71-Gb/s NRZ modulated 850-nm VCSEL-based optical link," *IEEE Photon. Technol. Lett.*, vol. 27, no. 6, pp. 577–580, Mar. 15, 2015.

[3] E. Haglund *et al.*, "30 GHz bandwidth 850 nm VCSEL with sub-100 fJ/bit energy dissipation at 25–50 Gbit/s," *Electron. Lett.*, vol. 51, no. 14, pp. 1096–1098, Jul. 2015.

[4] M. Liu, C. Y. Wang, M. Feng, and N. Holonyak, "850 nm oxide-confined VCSELs with 50 Gb/s error-free transmission operating up to 85 Â°C," in *Tech. Dig. Conf. Lasers Electro-Opt.*, San Jose, CA, USA, May 2016, pp. 1–3, Paper SF1L.6.

[5] J.-W. Shi, J.-C. Yan, J.-M. Wun, J. Chen, and Y.-J. Yang, "Oxide-relief and Zn-diffusion 850-nm vertical-cavity surface-emitting lasers with extremely low energy-to-data-rate ratios for 40 Gbit/s operations," *IEEE J. Sel. Topics Quantum Electron.*, vol. 19, no. 2, Mar./Apr. 2013, Art. no. 7900208.

[6] S. Imai *et al.*, "Recorded low power dissipation in highly reliable 1060-nm VCSELs for 'Green' optical interconnection," *IEEE J. Sel. Topics Quantum Electron.*, vol. 17, no. 6, pp. 1614–1619, Nov./Dec. 2011.

[7] G. Larisch, P. Moser, J. A. Lott, and D. Bimberg, "Impact of photon lifetime on the temperature stability of 50 Gb/s 980 nm VCSELs," *IEEE Photon. Technol. Lett.*, vol. 28, no. 21, pp. 2327–2330, Nov. 1, 2016.

[8] H. Hatakeyama *et al.*, "Highly reliable high-speed 1.1-$\mu$m-range VCSELs with InGaAs/GaAsP-MQWs," *IEEE J. Quantum Electron.*, vol. 46, no. 6, pp. 890–897, Jun. 2010.

[9] S. M. R. Motaghiannezam *et al.*, "180 Gbps PAM4 VCSEL transmission over 300 m wideband OM4 fibre," in *Proc. OFC*, Anaheim, CA, USA, Mar. 2016, pp. 1–3, Paper Th3G.2.

[10] D. M. Kuchta, "High capacity VCSEL-based links," in *Proc. OFC*, Los Angeles, CA, USA, Mar. 2017, pp. 1–2, Paper Tu3C.4.

[11] K. Szczerba *et al.*, "4-PAM for high-speed short-range optical communications," *IEEE/OSA J. Opt. Commun. Netw.*, vol. 4, no. 11, pp. 885–894, Nov. 2012.

[12] I-C. Lu *et al.*, "Very high bit-rate distance product using high-power single-mode 850-nm VCSEL with discrete multitone modulation formats through OM4 multimode fiber," *IEEE J. Sel. Topics Quantum Electron.*, vol. 21, no. 6, Nov./Dec. 2015, Art. no. 1701009.

[13] I-C. Lu *et al.*, "Ultra low power VCSEL for 35-Gbps 500-m OM4 MMF transmissions employing FFE/DFE equalization for optical interconnects," in *Proc. OFC*, Anaheim, CA, USA, Mar. 2013, pp. 1–3, Paper JTh2A.75.

[14] J.-W. Shi *et al.*, "Single-mode, high-speed, and high-power vertical-cavity surface-emitting lasers at 850 nm for short to medium reach (2 km) optical interconnects," *J. Lightw. Technol.*, vol. 31, no. 24, pp. 4037–4044, Dec. 15, 2013.

[15] K.-L. Chi *et al.*, "Single-mode 850-nm VCSELs for 54-Gb/s on–off keying transmission over 1-km multi-mode fiber," *IEEE Photon. Technol. Lett.*, vol. 28, no. 12, pp. 1367–1370, Jun. 15, 2016.

[16] A. Haglund, J. S. Gustavsson, J. Vukusic, P. Modh, and A. Larsson, "Single fundamental-mode output power exceeding 6 mW from VCSELs with a shallow surface relief," *IEEE Photon. Technol. Lett.*, vol. 16, no. 2, pp. 368–370, Feb. 2004.

[17] R. Safaisini, E. Haglund, P. Westbergh, J. S. Gustavsson, and A. Larsson, "20 Gbit/s data transmission over 2 km multimode fibre using 850 nm mode filter VCSEL," *Electron. Lett.*, vol. 50, no. 1, pp. 40–42, Jan. 2014.

[18] N. N. Ledentsov *et al.*, "Anti–waveguiding vertical–cavity surface–emitting laser at 850 nm: From concept to advances in high–speed data transmission," *Opt. Express*, vol. 26, pp. 445–453, Jan. 2018.

[19] J.-W. Shi, C.-C. Chen, Y.-S. Wu, S.-H. Guol, and Y.-J. Yang, "High-power and high-speed Zn-diffusion single fundamental-mode vertical-cavity surface-emitting lasers at 850-nm wavelength," *IEEE Photon. Technol. Lett.*, vol. 20, no. 13, pp. 1121–1123, Jul. 1, 2008.

[20] E. P. Haglund, P. Westbergh, J. S. Gustavsson, and A. Larsson, "Impact of damping on high-speed large signal VCSEL dynamics," *J. Lightw. Technol.*, vol. 33, no. 4, pp. 795–801, Feb. 15, 2015.

[21] P. B. Subrahmanyam, Y. Zhou, L. Chrostowski, and C. J. Chang-Hasnain, "VCSEL tolerance to optical feedback," *Electron. Lett.*, vol. 41, no. 1, p. 21, Oct. 2005.


**Zuhaib Khan** was born in Khalilabad, India in 1992. He received the Degree from the Department of Electronics and Communication Engineering, Jamia Millia Islamia, New Delhi, India. He is currently pursuing the Ph.D. degree with the Department of Electrical Engineering, National Central University, Taiwan. His current research interests include high-speed vertical-cavity surface-emitting lasers for application to optical interconnects.

**Jia-Liang Yen** was born in Kaohsiung, Taiwan, in 1969. He received the M.S. and Ph.D. degrees in electrical engineering from National Taiwan University in 1998 and 2004, respectively. He is currently an Assistant Professor with the Department of Information Technology, Takming University of Science and Technology, Taiwan. His research interests include vertical-cavity surface-emitting laser cavity design, cloud computing, and artificial intelligence, especially the power control of cloud systems.

**Chen-Lung Cheng** was born in Taipei, Taiwan, in 1995. He received the Degree from the Department of Electrical Engineering, Tunghai University. He is currently pursuing the master's degree with the Department of Electrical Engineering, National Central University, Taoyuan City, Taiwan. His current research interests high-speed vertical-cavity surface-emitting lasers.

**Kai-Lun Chi** was born in New Taipei City, Taiwan, in 1988. He is currently pursuing the Ph.D. degree with the Department of Electrical Engineering, National Central University, Taoyuan City, Taiwan. His current research interests include high-speed optoelectronic device measurement and high-speed vertical-cavity surface-emitting lasers and LEDs for optical interconnect applications.

**Jin-Wei Shi** (M'03–SM'12) was born in Kaohsiung, Taiwan, in 1976. In 2003, he joined the Department of Electrical Engineering, National Central University, Taoyuan City, Taiwan. From 2011 to 2012 and from 2016 to 2017, he was a Visiting Professor with the Electrical and Computer Engineering Department, UCSB. Since 2011, he has been a Professor with the Department of Electrical Engineering, National Central University. He has authored or co-authored over four book chapters, 130 journal papers, and 180 conference papers. He holds 30 patents. His current research interests include ultra-high speed/power photodetectors, electro-absorption modulator, terahertz photonic transmitter, and vertical-cavity surface-emitting lasers. He was a recipient of the Da-You Wu Memorial Award in 2010.